JOINTS IN POROUS ASPHALT CONCRETES: DENSITY AND TEXTURE SINGULARITIES

Praticò F. G.
Associate Professor – DIMET Department – Mediterranea University of Reggio Calabria – filippo.pratico@unirc.it
Moro A.
Research Assistant – DIMET Department – Mediterranea University of Reggio Calabria – antonino.moro@unirc.it
Ammendola R.
Research Assistant – DIMET Department – Mediterranea University of Reggio Calabria – rachele.ammendola@unirc.it

ABSTRACT

Nowadays we are demanding more performance from our pavements than ever before.

On the other hand, because of the difficulty in compacting the unconfined edges, lower density zones can occur at the longitudinal joints in HMAs (Hot Mix Asphalts); these joints can deteriorate faster than other areas and this contributes to the ultimate performance, then to pavement life and life cycle cost. Moreover, this problem may have a special role in Porous European Mixes (PEMs).

In the light of above facts, the objectives of this paper were to conduct a literature review on the above-specified topic and to investigate on density and texture-related issues in the joint area, for PEMs.

In order to pursue the objectives, in-lab and on-site experiments were designed and performed. On the basis of the obtained results, specific findings have been drawn.
Keywords: joint, Porous European Mixes, specific gravity

1. BACKGROUND AND MODELING

As is well known, in the longitudinal joints of HMAs local singularities in terms of density and surface texture are often detected. This can cause a decreased level of performance [AA.VV., 2003; AA.VV., 2004; AA.VV., 2006] and can modify pavement life cycle (see figure 1).

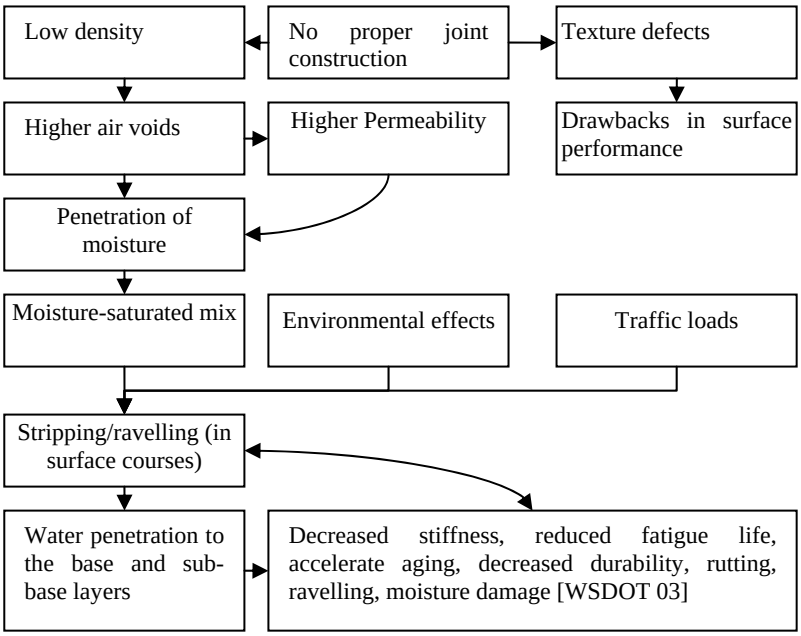

Figure 1 Joint density and related phenomena

Because of the difficulty in compacting the unconfined edges, lower density zones can anyway occur at the joints and this problem may have a special role in porous asphalt concretes.

On the basis of the analysis of the international literature on longitudinal joints [Kandhal P.S. et al., 2002; Kandhall and Mallik, 1996; Kandhall and Mallik, 1997; Sebaaly and Barrantes, 2004; Sebaaly P.E. et al., 2005; Sebaaly et al., 2005], it is possible to observe that construction process is affected by many factors. Table 1 summarises the main parameters of the problem. Paving technique, joint features and compaction strategy rule the quality level of the joint. Investigation may be based on visual inspection (surface defects), but joint density measurements are needed in order to estimate density levels and to assess if requirements are fulfilled.

Table 1 Joint construction: main parameters of the problem

Paving technique	Eliminate the joint altogether (if possible); Echelon paving; Proper mat overlap
Joint construction devices and	Cutting wheel (it cuts 25-50 mm of the unconfined, low density edge of the initial lane - cold lane - after compaction, while the mix is still plastic); Joint maker (raking is eliminated though a boot-like device);

geometry	Edge restraining device (it pinches the unconfined edge of the first lane towards the drum providing lateral resistance during the first roller pass); Tapered-notched; Tapered; Cut.
Joint adhesion	Heat the cold side before placing the hot side Coat the cold side with an adhesive material
Compaction	Environmental Factors (Temperature, Ground temperature, Air temperature, Wind speed, Solar flux); Mix Property Factors: Aggregate (Gradation, Size, Shape, Fractured faces, Volume, etc.), Asphalt Binder; Construction Factors (Rollers Type, Number, Speed and timing, Number of passes, Lift thickness, Others).
Rolling technique for the hot lane (initial roller pass technique)	Rolling from the hot side 150mm away from the joint (vibratory mode) Rolling from the hot side with overlapped onto the cold lane by about 150mm (vibratory mode) Rolling from the cold side (static mode)
Construction Problems	Surface Irregularities (Segregation, ravelling); Low Density
Joint density determination	Cores; Nuclear density gauges; Electric density gauges; Others
Indicators for joint specifications	- Air voids %(nuclear density gauges, typical acceptance range:8-11%) ; - %relative density (=100*joint density/pavement density; typical thresholds: <93% - poor; 93 to 97 – fair; >97, good); - %TMD (=100*joint density/pavement Theoretical Maximum Density; typical thresholds: >91%, 92%); - % lab density (=100*joint density/lab density; typical thresholds: 94-98%); pavement Theoretical Maximum Density Difference; - %corresp.mat.density

In figure 2 a simple theoretical model for density variation, here formalised, is shown; five zones are represented: i) 1-2: transition from the borderline of the Hot Lane (BHL) to the Undisturbed area of the HL (UHL); ii) 2-3: area of the UHL; iii) 3-4: transition from the UHL to the BCL (beyond the Joint J); note that the points 1 and 4 are predicted to be minima for G_{mb} function; in this zone the following indicators are here introduced:

$$\Delta G_{mb} = G_{mb}(x_4) - G_{mb}(x_3) \quad \text{(Eq.1)}$$

$$\Delta x = x_4 - x_3 \quad \text{(Eq.2)}$$

$$\Delta G_{mb}\% = 100 \cdot [G_{mb}(x_4) - G_{mb}(x_3)] / G_{mb}(x_3) \quad \text{(Eq.3)}$$

$$\partial G_{mb} / \partial x \cong \Delta G_{mb} / \Delta x \quad \text{(Eq.4)}$$

iv) 4-5: transition from BCL to UCL; v) 5-6: area of the UCL (the point 6 is not represented); vi) 6-7: transition from UCL to another BCL (not in joint, not represented); points 6 and 7 are not represented in figure 2.

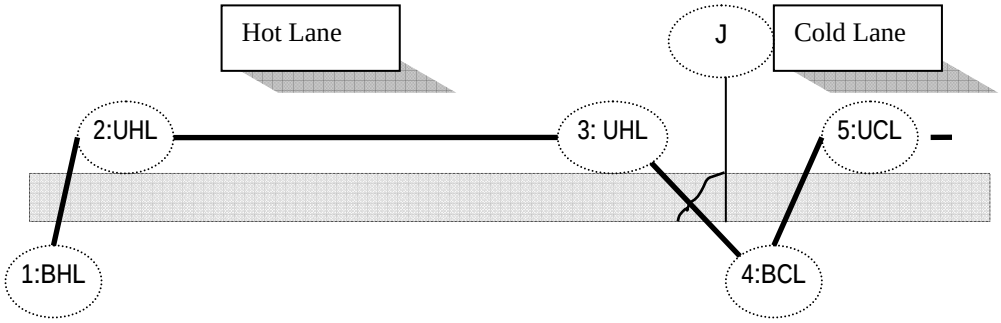

Figure 2 Simplified model for Specific Gravities variations (see tables 2 and 3)

According to some authors [AA.VV., 2006, - TRB Circular Number E-C105], for dense-graded friction courses, the main parameters of the transition zones near the longitudinal joint (point 4 in figure 2) can be described in terms of variation of a function $G_{mb}(x)$, where G_{mb} is a specific gravity, while x is the abscissa:

$\Delta G_{mb} = G_{mb}(x_4) - G_{mb}(x_3) \cong -0.13$;

$\Delta x = x_4 - x_3 \cong 10$cm (affected by the conventional determination of G_{mb} through cores extraction);

$\Delta G_{mb}\% = 100 \cdot [G_{mb}(x_4) - G_{mb}(x_3)] / G_{mb}(x_3) \cong -5.3$;

$\Delta G_{mb} / \Delta x \cong -0.01$ cm^{-1}.

Once formalised the model, the objectives and scope have been confined to the investigation on density and texture-related issues in the joint area, for Porous European Mixes (PEM). In particular, by referring to the different distance from the shoulder, the transverse variability of density has been analyzed. In order to pursue the objectives, in-lab and on-site experiments were designed (next section) and performed (§3). On the basis of the obtained results, specific observations and findings have been drawn.

2. TEST PLAN

The Factorial plan of the phase of the experiments referred in this paper is summarised in table 2. Additionally, the main boundary parameters above highlighted (table 1) are here specified.

Table 2 A summary of the experiments performed in the 1st phase

PHASE 1								
Joint Geometry: wedge								
Joint Construction devices: any								
Rolling Technique for the hot lane (initial roller pass technique): Rolling from the hot side 150 mm circa away from the joint								
Paving Technique: Proper mat overlap								
Roller: Steel roller, 80KN								
	E+M=HL			**J**		**M+S=CL**		**Tests**
	BHL	**UHL**	**CJ=UHL**	**J**	**JWS**	**BCL**	**UCL**	
29 cores	4	12	1	4	0	4	4	G_{mbgeom} G_{mb}, G_{mbAO}, n_{eff}, %b, G

12 MP	4	4	4	SH

Symbols. E+M= Emergency lane +driving lane; MP: Measurement Points; M+S=driving lane +Overtaking lane; J=Joint; UHL=Undisturbed Hot Lane; UCL=Undisturbed Cold Lane; BCL=Borderline between HL and CL but within the Cold Lane; SH= Sand Height; G_{mbgeom}: mix bulk specific gravity (dimensional method, AASHTO T 269); G_{mb}=mix bulk specific gravity (vacuum seal method, ASTM D6752; ASTMD6857); G_{mbAO}=mix bulk specific gravity after opening (vacuum seal method, ASTM D6752; ASTMD6857); n_{eff}=mix effective porosity (ASTM D6752; ASTMD6857); JWS= Joint with asphalt binder spot.
Note: The MPD (Mean Profile Depth) has been derived from SH according to PIARC experiment [AA.VV., 1995].

Figures 3 and 4 show the main phases of the field compaction process:
1) laydown and compaction of the Cold Lane;
2) laydown and compaction of the Hot Lane. In this phase rolling from the hot side with overlapping onto the cold lane by about 150mm has been carried out.
After the construction of the so-called Cold Lane (CL) and Hot Lane (HL) (see figures 2 to 4), in-site (SH, etc.) and in-lab (on the extracted cores) measurements have been performed. Locations have been divided into six main classes, depending on the predicted level of "borderline singularity" (BHL, UHL, J, JWS, BCL, UCL, see table 2). The following parameters have been determined on the extracted cores (see figure 5): *b (%)* = asphalt binder content as a percentage of aggregate weight (B.U. CNR n.38/73; ASTM 6307); *G* = aggregate gradation (B.U. CNR n. 4/53); γ_g = aggregate apparent specific gravity (B.U. CNR n. 63/78); G_{mb} = mix bulk specific gravity (ASTM D6752; ASTM D6857); G_{mbAO} = mix bulk specific gravity after opening (ASTM D6752; ASTM D6857); n_{eff} = mix effective porosity (ASTM D6752; ASTM D6857) (see Figure 5). The effective porosity (n_{eff}) has been calculated from G_{mb} and G_{mbAO}: $n_{eff}=(G_{mbAO}\cdot\gamma_w - G_{mb}\cdot\gamma_w)\cdot(G_{mbAO}\cdot\gamma_w)^{-1}$, γ_W = water density.

Figure 3 Cold lane compaction

Figure 4 Hot lane compaction

		
Extraction: b(%) (CNR n. 38/73; ASTM 6307)	Sieves, screens, sieve shaker: G (CNR n. 4/53)	Vacuum Sealing: G_{mb}, G_{mbAO}, n_{eff} (ASTM D6752; D6857)

Figure 5 Main devices used

3. RESULTS AND ANALYSIS

Tables 3 and 4 and figures 6 to 19 summarize the obtained results.

Table 3 Main results

Section	Core	Lane	Position	Distance (cm)	$G_{mb\ geom}$	SH	$G_{mb\ corelok}$	G_{mbAO}	n_{eff} (%)
1	c6	E+M	BHL	13	1,712		1,936	2,666	27,37
1	c5	E+M	UHL	63	1,671	3,46	1,941	2,647	26,66
1	c4	E+M	UHL	113	1,722		1,917	2,659	27,92
1	c3	E+M	UHL	163	1,752		1,973	2,694	26,79
1	cj	E+M	UHL	213	1,849		1,995	2,664	25,11
1	cg	J	J	487,5	1,690	2,83	1,912	2,650	27,86
1	c8	M+S	BCL	495	1,695		1,890	2,687	29,66
1	c9	M+S	UCL	515	1,691	3,32	1,877	2,694	30,32
2	c6	E+M	BHL	13	1,767		1,923	2,645	27,32
2	c5	E+M	UHL	63	1,868	2,89	2,010	2,620	23,31
2	c4	E+M	UHL	113	1,842		1,997	2,560	21,98
2	c3	E+M	UHL	163	1,901		2,038	2,607	21,81
2	cg	J	J	487,5	1,836	1,79	1,987	2,678	25,82
2	c8	M+S	BCL	495	1,745		1,918	2,683	28,51
2	c9	M+S	UCL	515	1,832	2,12	1,983	2,664	25,57
3	c6	E+M	BHL	13	1,760		1,917	2,677	28,40
3	c5	E+M	UHL	63	1,706	2,92	1,902	2,626	27,55
3	c4	E+M	UHL	113	1,682		1,932	2,627	26,44
3	c3	E+M	UHL	163	1,793		1,959	2,580	24,07
3	cg	J	J	487,5	1,806	2,41	1,972	2,606	24,31
3	c8	M+S	BCL	495	1,816		1,958	2,637	25,74
3	c9	M+S	UCL	515	1,860	2,83	1,994	2,706	26,33
4	c6	E+M	BHL	13	1,869		2,028	2,545	20,33
4	c5	E+M	UHL	63	1,903	3,19	1,978	2,584	23,45
4	c4	E+M	UHL	113	1,844		1,979	2,610	24,15
4	c3	E+M	UHL	163	1,905		2,020	2,604	22,43
4	cg	J	J	487,5	1,749	1,96	1,952	2,632	25,83
4	c8	M+S	BCL	495	1,794		1,943	2,663	27,03
4	c9	M+S	UCL	515	1,775	3,19	1,971	2,681	26,49
SYMBOLS: see table 2									

Figures 6 to 13 show the variations of G_{mbgeom}, G_{mb} (vacuum sealing device) and n_{eff} for different distances from the shoulder.

Note that a vertical line (bolded) is reported at the abscissa 487.5 cm: it represents the joint position and divides the hot lane (HL, on the left) from the cold lane (CL, on the right).

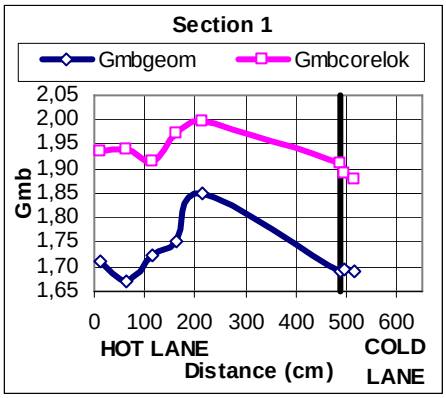

Figure 6

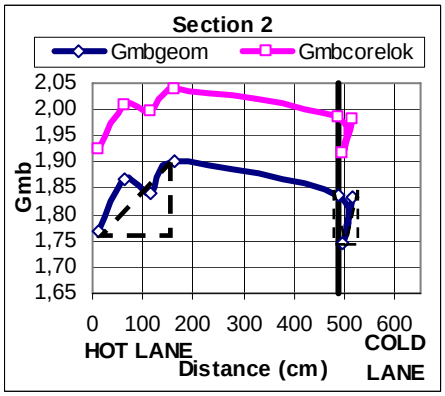

Figure 7

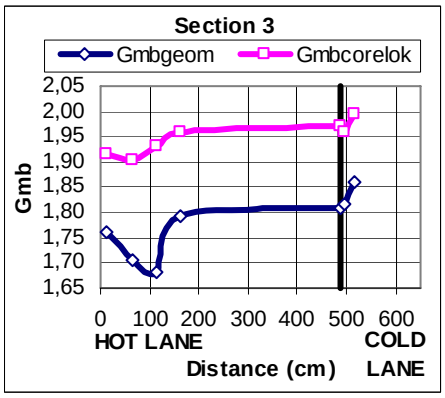

Figure 8

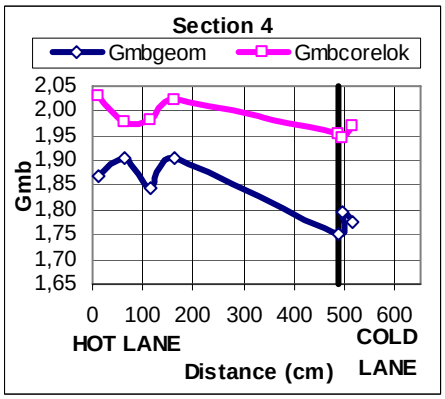

Figure 9

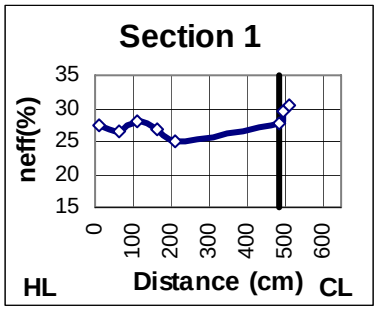

Figure 10

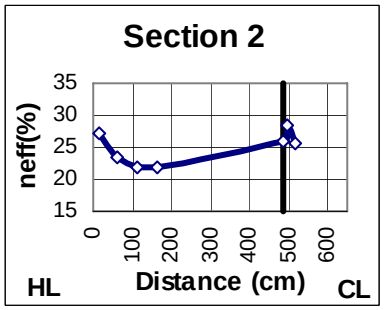

Figure 11

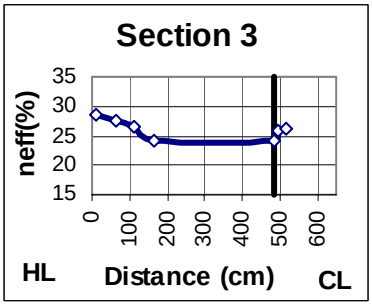

Figure 12

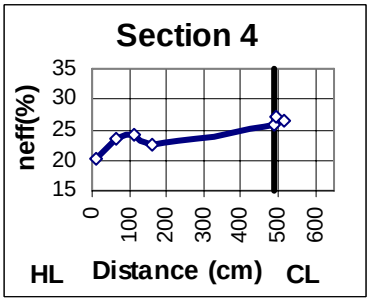

Figure 13

Table 4 summarises the comparison between the simplified model above-described for G_{mb} variations and the obtained results. By referring to figures 6 to 13 and table 4, the following observations may be remarked:

1. statistic robustness of the experiments and of the obtained data base needs to be optimised due to the low number of cores and experiments analysed; this fact could affect the generality and the reliability of some of the observations that follow. Moreover, many sources of variability affect the data base. Note that each value of G_{mb} originates from only one measurement. Therefore variance is affected both by spatial variability (longitudinal and transverse) and errors in measuring HMA density;
2. the zone1-2 (see figure 2) seems to have an extension contained in less than 100cm; in this zone the G_{mb} often increases while the effective porosity decreases (see table 4);
3. in the zone 2-3 density variations could be due only to heterogeneity in material or in construction variables;
4. in the transition zone 3-4 G_{mb} often decreases while the effective porosity increases;
5. in the transition zone 4-5 G_{mb} often increases while the effective porosity decreases;
6. it is recurrent the presence of a local minimum at about 100 cm from the guard-rail (i.e. from the BHL point on the left); more research is needed on the possible causes;

7. specific gravities are not always well-correlated; by referring to errors in measuring HMA specific gravity, there is a well-known problem of intrinsic correlation between G_{mbgeom} and G_{mb} (Vacuum sealing device); it must be remarked that G_{mbgeom} is greatly affected by core integrity;
8. many points do not agree with the simple model above-formalised; some of them are suspected to be outliers; in particular, in section 1 (figure 6) and 4 (figure 9), there are possible outliers among BHL points; in section 3 (figure 8) there are possible outliers among BCLs;
9. the hypothesis of homogeneity of material and of construction procedures, which supports a common G_{mb} (and n_{eff}) value for UCL and UHL could be too strong; this fact may be the reason of some of the detected variations in G_{mb} behaviour; more research is needed on this topic;
10. it is interesting to observe that the density gap in the transitions boundary-body 3-4 is sometimes quite conforming to other experimental investigations; in fact, for dense-graded friction courses, DGFC ([AA.VV., 2006], TRB Circular 105), percent density gaps (Eq.3) are around -5.3% vs -3.8~-5.3% obtained for the investigated PEMs; density gaps (Eq.1) are around -0.13, vs -0.08~-0.10 for the investigated PEMs; this could mean a 3~4% more in air voids content in BCL; is there a difference between PEMs and DGFCs? Can requirements be the same? More research is needed, but first results reported in table 4 are quite encouraging.

Table 4 Tentative characterization of the model

section	zone	$\Delta G_{mb\ geom}$ (%)	ΔG_{mb} (%)	Δn_{eff} (%)
1	1--2	7,4	3,0	-9,0
2	1--2	7,0	-1,5 (⊗)	-25,3
3	1--2	1,8	-3,8 (⊗)	-18,0
4	1--2	1,9	2,3	9,4 (⊗)
all	1--2	3,6	-1,0 (⊗)	-11,3
1	3--4	-8,3	-5,3	18,1
2	3--4	-8,2	-5,9	30,7
3	3--4	1,3 (⊗)	-0,1	6,9
4	3--4	-5,8	-3,8	20,5
all	3--4	-5,3 (*)	-3,8 (*)	19,1
1	4--5	-0,2 (⊗)	-0,7 (⊗)	2,2 (⊗)
2	4--5	5,0	3,4	-10,3
3	4--5	2,4	1,8	2,3 (⊗)
4	4--5	-1,1 (⊗)	1,4	-2,0
all	4--5	1,5	1,5	-1,9

(⊗):this result doesn't conform to the above formalised model.
(*): for DGFCs a value of -5.3% has been obtained (TRB Circular 105, [AA.VV., 2006]).

Finally, figures 14 and 15 show texture variations for the selected points; just a few measurements have been performed. However, it is possible to observe that the negative correlation between G_{mb} and MPD (mm) doesn't seem always to be confirmed, probably due to local effects/spots (see figure 15).

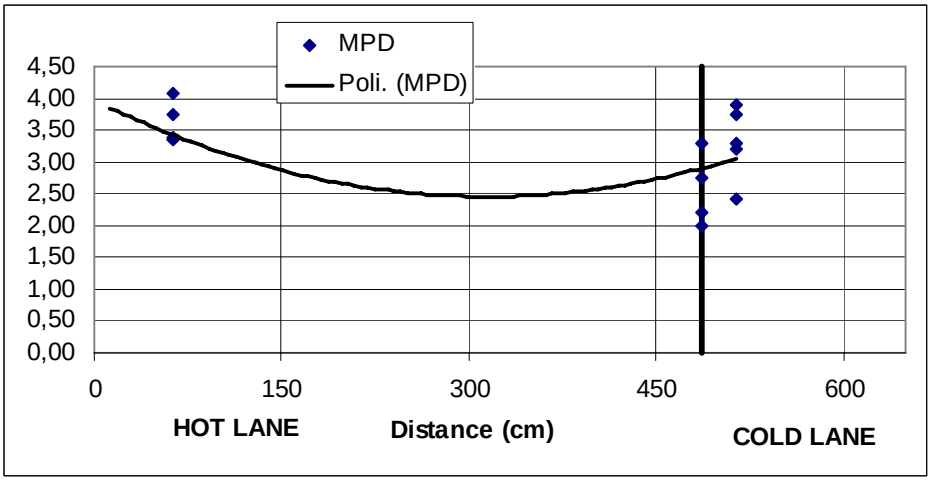

Figure 14

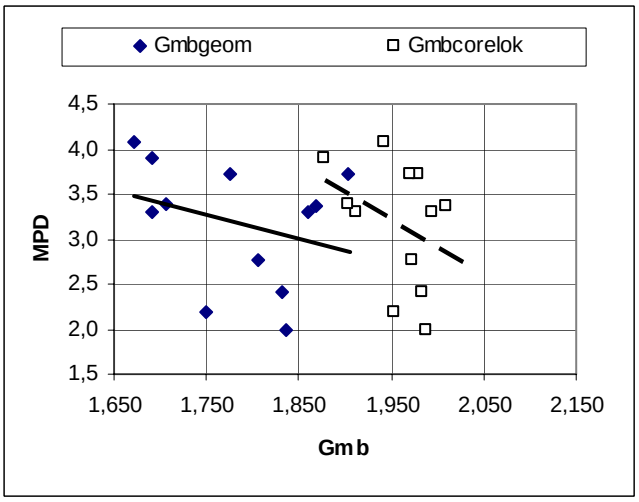

Figure 15

4. FUTURE RESEARCH

First experiments confirmed that variations due to material and construction variability greatly affect the collected data base.

Though this, first results encourage to carry on more research and to complete the analysis of the collected data, in order to allow data to be more robust and so observations more reliable.

During the 2nd phase of experiments and analyses, data collected on the same sections by a non nuclear density gauge will be analysed together with other performance indicators.

By crossing over cores data and non nuclear portable gauge data (more points, lower steps) analyses will aim to support, optimise or discard the above-formalised model.

5. MAIN FINDINGS

The following main findings can be drawn:

a) factor affecting density and texture for longitudinal joints of PEMs appear to be numerous and a large number of experiments is needed in order to mitigate "noise" in data analysis;
b) the formalised model, in which three minima are predicted (BCL, BHL, and another BHL in the other shoulder), could be too simple to explain a so complex process in which many sources of variability are merged (materials, layers and construction variability, weather conditions during compaction of HL and CL, etc.);
c) more research is needed on many of the above-mentioned topics;
d) the variations of the effective porosity are often quite appreciable and consistent; this seems to support the interpretation of ravelling phenomena in longitudinal joints, especially when they are bad-positioned (near wheel tracks);
e) density and specific gravity variations seem to be quite similar to that recorded by other authors on DGFC; though more research is needed, this could support similar acceptance criteria for longitudinal joints in PEMs;
f) when SH variability is concerned, it is possible to observe that transverse variability, longitudinal variability and joint singularities could be three synergetic sources of variance, but other research is needed on this topic and the use of more precise and accurate devices could make the difference;
g) future research will aim to mitigate the influence of the involved boundary conditions in order to make it possible to pursue more reliable inferences.

REFERENCES

AA.VV. (1995) - International PIRC experiment to compare and harmonise texture and skid resistance measurements, PIARC, France, 1995.

AA.VV. (2003) - Longitudinal Joint Construction techniques, Tech Notes, Washington State Department of Transportation, February 2003.

AA.VV. (2004) – TRB of the National Academies, National Cooperative Highway Research Program, Quality characteristics for use with performance-related specifications for hot mix asphalt, Research Result Digest 291, August 2004.

AA.VV. (2006) - TRB Circular Number E-C105, Transportation Research Board, General Issues in Asphalt Technology Committee, Factors Affecting Compaction of Asphalt Pavements, September 2006.
KANDHAL P.S., RAMIREZ T.L., INGRAM P.M. (2002) - Evaluation of eight longitudinal techniques for asphalt pavements in Pennsylvania, National Center for Asphalt Technology Report No 02-03, February 2002.
KANDHALL P.S., MALLIK R.B. (1996) - A study of longitudinal Joint Construction techniques in HMA pavements (interim report – Colorado project), National Center for Asphalt Technology Report No 96-03, August 1996.
KANDHALL P.S., MALLIK R.B. (1997) - Longitudinal Joint Construction techniques for asphalt pavements, National Center for Asphalt Technology Report No 97-04, August 1997.
SEBAALY P.E. AND BARRANTES J.C. (2004) - Development of a joint density specification: phase I: literature review and test plan, Western Regional superpave center, Nevada Department of Transportation, Carson City, NV, USA, 2004.
SEBAALY P.E. AND BARRANTES J.C., FERNANDEZ G. (2005) - Development of a joint density specification: phase II: evaluation of test sections, Nevada Department of Transportation, Carson City, NV, USA, 2005.
SEBAALY P.E., BARRANTES J.C., FERNANDEZ G., LORIA L. (2005) - Development of a joint density specification: phase II: evaluation of 2004 and 2005 test sections, Nevada Department of Transportation, Carson City, NV, USA, December 2005.